AIChE

Molecular Mechanisms Responsible for the Structural Changes Occurring During Geopolymerization: Multiscale Simulation

Claire E. White
Dept. of Chemical and Biomolecular Engineering, University of Melbourne, Victoria 3010, Australia

Lujan Neutron Scattering Center, Los Alamos National Laboratory, NM 87545

Center for Nonlinear Studies, Los Alamos National Laboratory, NM 87545

John L. Provis
Dept. of Chemical and Biomolecular Engineering, University of Melbourne, Victoria 3010, Australia

Thomas Proffen
Neutron Scattering Science Center, Oak Ridge National Laboratory, TN 37831

Jannie S. J. van Deventer
Dept. of Chemical and Biomolecular Engineering, University of Melbourne, Victoria 3010, Australia

DOI 10.1002/aic.12743
Published online September 1, 2011 in Wiley Online Library (wileyonlinelibrary.com).

To date, the fundamental details of the molecular structural changes and associated mechanisms, which take place during the formation of aluminosilicate geopolymer gels, have remained largely elusive. Here, density functional theory-based coarse-grained Monte Carlo modeling, a multiscale simulation technique, is used to simulate the geopolymerization reaction and to determine the molecular mechanisms controlling this process. Silica supplied by the alkaline solution plays a significant role in enhancing the dissolution of the solid aluminosilicate precursor (metakaolin, in this case) and the polymerization of the gel. In the reaction between NaOH and metakaolin, in the absence of initially dissolved silica, the solid precursor completely dissolves and the aluminosilicate gel forms via the percolation of small aluminosilicate clusters. On the other hand, in the presence of dissolved silicate, the metakaolin only partially dissolves, as the aluminosilicate gel precipitates on the surfaces of the metakaolin particle after a period of time. *AIChE J,* 58: 2241–2253, 2012
Keywords: coarse-graining, Monte Carlo, geopolymerization, density functional theory, aluminosilicates

Introduction

Geopolymers are a class of inorganic polymer cement typically synthesized via alkaline activation of aluminosilicate precursors. Geopolymer binders display similar mechanical properties to traditional ordinary Portland cement while requiring approximately 80–90% less CO_2 in production, which makes these materials a viable and attractive alternative to traditional cements in numerous industrial settings.[1] Nevertheless, there remain outstanding questions regarding the structural development and durability of this new class of material, which can only be addressed using advanced experimental and simulation techniques. Here, the structural changes occurring during formation of geopolymer gels are investigated using a recently introduced multiscale simulation methodology,[2] providing new insight into the structural mechanisms responsible for the formation of this technologically important material.

The complexity of aqueous aluminosilicate chemistry, including the various processes occurring concurrently during a solid–liquid reaction process such as geopolymer synthesis, makes simulation of the complete system inherently difficult.[3] In fact, the exact details of the process of conversion from an aluminosilicate precursor in alkali media to a geopolymeric gel have yet to be confirmed experimentally or theoretically, due to the highly complex nature of this process.[4] There have been several models proposed regarding the mechanisms responsible for alkali activation of various materials, and these mechanisms have been utilized to aid explanation of geopolymerization, mainly based on the early work of Glukhovsky on alkali-activation of metallurgical slags.[5] Building on these mechanistic details, Duxson et al.[4] described a highly simplified reaction mechanism for geopolymerization, and Provis and van Deventer[3] developed a corresponding multistep reaction kinetic model derived from previous geochemical reaction process modeling. During geopolymerization, the aluminosilicate precursor (usually metakaolin or fly ash; metakaolin is specifically studied here) dissolves into a highly alkaline solution (sometimes containing additional soluble silica), releasing aluminate and silicate monomers. These monomers then undergo condensation reactions to move the

Additional Supporting Information may be found in the online version of this article.

Correspondence concerning this article should be addressed to J. L. Provis at jprovis@unimelb.edu.au.

system towards equilibrium. Subsequently, the supersaturated aluminosilicate solution undergoes gelation, forming the initial gel phase (denoted *gel 1*). Over time, this gel is observed to reorganize via reactions mediated by the alkaline environment of its pore solution, to form a more crosslinked gel (denoted *gel 2*). Many of these processes occur to some degree simultaneously, with dissolution of the aluminosilicate source occurring in parallel with repolymerization of silicate and aluminate species, making experimental characterization of the individual processes challenging, if not impossible.[3]

Previous investigations modeling the geopolymerization process[3,6,7] have elucidated important reaction details but do not provide accurate molecular-level mechanistic information, such as cluster size distribution profiles and aluminosilicate dissolution behavior. Other investigations have attempted to reproduce the molecular processes occurring during geopolymerization[8,9] but did not account for the solution chemistry environment present during geopolymerization and are therefore somewhat limited in applicability.[10] Hence, there is a void in the literature regarding detailed mechanistic modeling of the geopolymerization reaction.

More generally, there have been numerous theoretical and experimental investigations into silicates and aluminosilicates at the atomistic level (dissolution and growth mechanisms), enabling clarification of the individual processes, which are predominantly responsible for the overall behavior of this general class of materials.[11–19] However, the individual theoretical models fail to replicate the complete mesoscopic and microscopic behaviors of a multiscale heterogeneous material, mainly due to the massive computational requirements associated with atomistic modeling across the necessary range of length scales. There are several types of modeling that have been used for these length scales, which have proven to be successful. Kinetic models have been used to simulate aluminosilicate dissolution[20] and geopolymerization.[3,7] Similarly, dynamic Monte Carlo simulations, using reaction rates of individual processes to determine the probabilities of events, have been used to simulate silica sol–gel chemistry.[21,22] However, dynamic Monte Carlo modeling requires an in-depth knowledge of the reaction rates of all the atomistic processes occurring, which is currently not available for geopolymerization.[3] Hence, application of an alternative form of Monte Carlo modeling, coarse-grained Monte Carlo (CGMC) modeling,[23,24] will be beneficial in simulating geopolymerization.

Previously, we simulated the initial stages of alkali silicate gel formation using a multiscale density functional theory (DFT)/CGMC methodology.[2] This novel methodology used the Gibbs free energies of dimerization of silicate species, calculated by density functional modeling,[25] as the interaction parameters on which the CGMC simulation was based. The simulation methodology required no empirical calibration, with silicate speciation results agreeing at least semiquantitatively with experimental ^{29}Si nuclear magnetic resonance (NMR) data for a wide range of silica concentrations at high alkalinity. Here, a similar methodology is applied to three metakaolin-based geopolymer systems with differing activating solutions (hydroxide-, hydroxide/silicate-, and silicate-activation of metakaolin) in order to elucidate the molecular mechanisms occurring in these systems. In addition to the silicate species used in the modeling of the silicate gels previously,[2] aluminate species and their interactions with small silicate species have also been described in recent density functional calculations,[25] and hence, aluminate monomers and associated dimerization energies are incorporated into the CGMC simulations for metakaolin-based geopolymer systems presented here. By modeling the individual nearest-neighbor interactions occurring in a geopolymer system and, therefore, accounting for the dominant reaction types (dissolution and condensation), this study addresses these previously unknown molecular mechanisms from a modeling viewpoint, answering critical outstanding questions regarding the process of geopolymerization.

Table 1. Gibbs Free Energies of Dimerization Reactions ($\Delta G_{reaction}$; kJ/mol) Occurring in an Aluminosilicate Solution at a pH of 11 (Ref. 25)

Monomer species	M	$M^-{\cdot}Na{\cdot}3H_2O$	$M^{2-}{\cdot}2Na{\cdot}6H_2O$	$A^-{\cdot}Na$
M	−1.8	−9.3	−5.3	−21.2
$M^-{\cdot}Na{\cdot}3H_2O$		−0.9	8.1	−9.7
$M^{2-}{\cdot}2Na{\cdot}6H_2O$			35.0	14.5
$A^-{\cdot}Na$				16.9

*M = $Si(OH)_4$, M^- = $SiO(OH)_3^-$, M^{2-} = $SiO_2(OH)_2^{2-}$, A^- = $Al(OH)_4^-$

Model Description

It should be noted that much of the DFT/CGMC methodology has already been discussed and justified in detail in our previous investigation of silicate systems.[2] Hence, for the sake of brevity, this information has not been reproduced in full here. However, there are important differences between the previous and current investigations, which have been outlined below, along with a brief summary of the model implementation.

Interactions between Species

This model simulates the formation of an aluminosilicate geopolymer gel from metakaolin, where the dissolution of metakaolin results in silicate and aluminate monomers in solution. These monomers then rearrange and participate in polymerization reactions to form the geopolymer gel. The most fundamental reaction in silica sol–gel chemistry is the dimerization of two neutral silicic acid species, $Si(OH)_4$, which react to produce a dimer, $(OH)_3SiOSi(OH)_3$, and a water molecule.[2] The cornerstone of the MC model presented here is the use of the energetics of this and other dimerization reactions involving silicate and aluminate monomers.

Table 1 reports the condensation reaction energies for dimerization of silicate and aluminate monomers, as calculated using density functional theory (DFT).[25] The total energy of the system is calculated as the sum of the relevant dimerization energies for all occupied sites in the lattice according to their bonding environments.

Swap and bond events

For the system to move toward equilibrium, two types of events can occur; a ''swap'' event or a ''bond'' event. One iteration is defined as one swap or bond event and acceptance of an event is determined using a biased sampling algorithm based on the Boltzmann factor and the configurational change.[2,26] A swap event entails selecting at random one occupied site (silicate or aluminate, bonded or nonbonded) and another site (occupied or unoccupied), with acceptance of this event determined according to the Metropolis algorithm. A bond event entails selecting an occupied site (bonded or nonbonded) at random and seeing whether it has any nonbonded occupied neighbors. If so, the

Table 2. Equilibrium Constants for Silicate Speciation, Obtained from the Literature as Noted

Species	pK_a^1	pK_a^2	pK_a^3
Q^0 (monomer)	9.5[27]	12.6[27]	15.7[27]
Q^1 (dimer)	9.85[27]*	13.25[27]*	16.65[27]*
Q^2	11.2[28]	13.1[29]	–
Q^3	11.2[28]	–	–

*pK_a^1 is the average of the first and second pK_a values of the dimer ($pK_{a,d}^1$ and $pK_{a,d}^2$), pK_a^2 is the average of $pK_{a,d}^3$ and $pK_{a,d}^4$ in that paper, and pK_a^3 is the average of $pK_{a,d}^5$ and $pK_{a,d}^6$.
†pK_a^2 is the average of the values of pK_a^4, pK_a^5, and pK_a^6 for a trimer.

site and its neighbor site are updated to "bonded" with a probability determined according to the biased sampling algorithm. The two functions are called in an alternate fashion (i.e., swap, bond, swap, bond, and so on), so that 50% of trialed events are carried out using the swap function, the other 50% using the bond function.

It should be noted that the model does not describe any change in the reactivity of a site depending on whether or not it is already bonded to other sites; the energy change associated with a site bonding to another site is calculated using the Gibbs free energy of dimerization of two monomeric species,[25] irrespective of the existing bonding environment of the sites involved. This does not precisely represent the case for a real system because the pK_a of a silicate site is known to depend on its connectivity,[27] and so it would be expected that the Gibbs free energy of bond formation would similarly be expected to change. However, if this was a significant limitation in the simulation methodology, it would be anticipated to become apparent in the results obtained.

Silica deprotonation

The influence of silica deprotonation and its implementation in the DFT/CGMC methodology have been discussed extensively in our previous investigation.[2] The deprotonation constants of silicate sites of different connectivity are reproduced in Table 2 for completeness. Deprotonation of aluminate is not considered in this work, as it requires a much higher pH than is achieved during geopolymerization.[10] Simulations were carried out at a constant pH of 11 because the simulation methodology was implemented using a constant pH value, and a pH of 11 is the closest approximation for the range of geopolymer gels investigated over the extent of reaction.

Metakaolin dissolution

The DFT/CGMC model describes aluminosilicate precursor dissolution through inclusion of a metakaolin particle within the simulation box at the start of a simulation, which is then subjected to the MC moves as described above, in exactly the same way as the remainder of the simulation box. The metakaolin particle is modeled as a cube consisting of alternating silica and alumina layers, where silicate sites are initially neutral, and each species is defined as fully bonded, as the structural nature of this material is known to retain the layered alumina and silica sheets found in its parent material kaolinite. The conversion from kaolinite to metakaolin (usually calcining at temperature between 550 and 750°C) and associated removal of hydroxyl groups results in alumina layers (and to a lesser extent the silica layers) that are highly strained and buckled, which leads to a chemically reactive amorphous phase.[30–32] The bonding environment has been altered from that which is applied throughout the rest of the system to enable the presence of six-coordinated sites within the unreacted metakaolin particle, which greatly simplifies its implementation. Obviously, this simplification deviates from a perfectly accurate representation of the silicon and aluminum coordination environments in metakaolin; in reality, metakaolin contains four-coordinated silicon sites and a distribution of three-, four-, and five-coordinated aluminum.[30–32]

However, the manner in which metakaolin is represented in this MC model will at least semiquantitatively replicate the results seen experimentally during dissolution. The range of coordination states in which aluminum is present in metakaolin indicates the high degree of strain present in the alumina layers, meaning that they readily dissolve into alkaline solutions. On the other hand, the silicon atoms are mainly in fourfold coordination, and therefore, the silica layers tend to be less reactive.[20] From Table 1, the bonded aluminate monomers forming the alumina layers will be expected to dissolve preferentially due to the highly unfavorable nature of the aluminate dimerization reaction (i.e., two bonded aluminate sites will prefer to break apart from each other). The silica layers consist of bonded neutral silicate sites, for which the condensation reaction is slightly favorable (Table 1). The strongest bonds within the metakaolin particle are those between silica and alumina layers; Table 1 shows that the dimerization reaction between an aluminate monomer and a neutral silicate monomer is strongly favorable. This will obviously impact the manner in which metakaolin dissolves. However, it is only by comparison of simulation results with existing knowledge regarding metakaolin dissolution that it will be possible to determine whether the description of metakaolin is successful.

Simulation details

Monte Carlo simulations have been conducted in the canonical ensemble (NVT; constant number of occupied sites, system volume and temperature). The simulations were conducted as described in our previous investigation;[2] however, there is one major difference required due to the inclusion of metakaolin in the system. In the synthesis of a metakaolin-based geopolymer, the alkaline solution is usually left to equilibrate prior to addition of metakaolin, which for the case of silicate solutions means that silica oligomers will be present at the start of the reaction process. Hence, the DFT/CGMC simulations of systems containing initially dissolved silica were subjected to a preliminary equilibration procedure, where only MC moves involving sites not contained in the metakaolin particle were allowed to be accepted, leaving the particle itself unchanged. Once the solution obtained equilibrium—after 1,000,000 iterations—the metakaolin particle was then allowed to participate in the process, and geopolymerization commenced. The point at which the metakaolin is "added" to the system is denoted iteration 0, with pre-equilibration taking place from iteration "−1,000,000" to iteration 0.

All simulations carried out in this investigation consist of a 125,000-site cubic lattice (50^3 sites) with periodic boundary conditions in all three Cartesian coordinates. Larger lattice sizes were investigated, and it was determined that this size (50^3 sites) provided a good balance between minimizing the artificial effects induced in small lattice simulations (refer to Figure 6 in Ref. 33) and obtaining convergence in a

Table 3. Compositions of the Geopolymer-Forming Systems Investigated

System*	Lattice site percentage (%)		
	Water + Na	Silica in solution	Metakaolin
Hydroxide-activated	76.4	0.0	23.6
Hydroxide/silicate-activated	72.2	5.6	22.2
Silicate-activated	68.4	10.6	21.0

*The hydroxide-activated system corresponds to a stoichiometry of $NaAlSiO_4 \cdot 5.5H_2O$ (metakaolin activated with NaOH), compared to $NaAlSi_{1.5}O_5 \cdot 5.5H_2O$ for the hydroxide/silicate-activated system (metakaolin activated with sodium silicate of modulus (molar ratio SiO_2/Na_2O) of 1.0), and $NaAlSi_2O_6 \cdot 5.5H_2O$ for the silicate-activated system (metakaolin activated with sodium silicate of modulus 2.0).

reasonable amount of time. It should be mentioned that the size of simulation used here is less than the size reported by Šomvársky and Dušek necessary to accurately replicate the infinite system (10^6–10^7 site simulations were the closest to replicating the real system), where kinetic Monte Carlo simulations were used to model network formation.[34,35] On the other hand, the investigation by Herrmann et al.,[36] which modeled irreversible gelation using a simple lattice approach ranging from 15^3 up to 60^3 sites, was capable of replicating the gelation phenomena using these smaller lattice sizes. Hence, the choice of 50^3 for the lattice size was deemed appropriate for the current investigation.

For each simulation, the energy of the system is recorded at regular intervals. Systems are allowed to equilibrate for 4,000,000 to 7,000,000 iterations, (in addition to pre-equilibration, where one iteration is defined as one trailed swap or bond event, accepted or rejected), until the energy reaches a constant value. During simulations, the configuration of the box contents is recorded periodically. Detailed analyses of cluster distributions during simulations are carried out using a flood technique to search the occupancy and bonding environment of all sites and therefore identify all clusters present in the simulation box. Cluster compositions (percentage silica and alumina) and bonding information (percentage of Si—O—Si, Si—O—Al, and Al—O—Al bonds) are also calculated from the saved configuration information.

Three geopolymer gels of differing compositions are investigated, each derived from the use of an alkaline solution with a different initial silica concentration, with metakaolin as the aluminosilicate source in all cases. The starting configuration of each simulation contains a metakaolin particle surrounded by the solution, with site percentages as displayed in Table 3.

Results and Discussion

For the systems described in Table 3, there were no significant changes in energy or structure when runs were continued for more than 4,000,000 (hydroxide (H) system) or 7,000,000 (hydroxide/silicate (H/S) and silicate (S) systems) iterations, indicating that equilibrium had been reached (refer to Supporting Information for the energy profiles of each system). This is a much longer equilibration period than was required for most of the sodium silicate solutions described in our previous investigation,[2] because of the higher percentage of occupied sites and therefore the greater number of individual events (bond and swap) needed for the systems to reach equilibrium here.

Monomer speciation

The distribution of dissolved silicate and aluminate species coexisting with developing geopolymer gels during their formation can provide important information regarding the mechanisms occurring during geopolymerization. Figures 1a and 1b display the percentage of occupied sites existing as silicate and aluminate monomers, respectively, at various stages during the simulations.

Figure 1a shows obvious differences between the systems investigated in terms of the silicate monomers present during the simulations. For the hydroxide-activated geopolymer gel (H), the initial percentage of silicate monomers is zero. As the extent of reaction progresses, this percentage increases (to 21.8% at 4,000,000 iterations), whereas for the silicate-activated geopolymer gel (S), the percentage of silicate monomers decreases slightly over time (from 21.9% at 0 iterations to 16.6% at 7,000,000 iterations). For the mixed system (H/S), the percentage of silicate monomers increases slightly throughout the entire reaction, from 16.0 to 19.0%. However, the final configurations each possess roughly similar percentages of silicate monomers, indicating that the silicate monomer concentration in the remaining solution (representing the pore solution of a hardened geopolymer binder) is similar for metakaolin-based geopolymer gels,

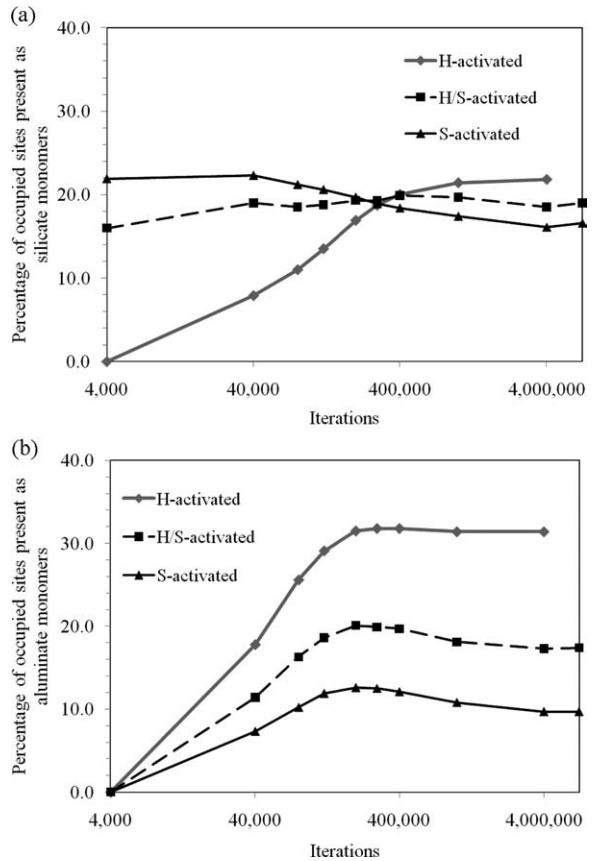

Figure 1. Percentage of occupied sites existing as (a) silicate monomers and (b) aluminate monomers at various stages during the simulations of geopolymer gels (H denotes hydroxide, S denotes silicate).

Note that iteration 0 (commencement of metakaolin dissolution) is displayed as iteration 4000 in the Figure, to enable use of a logarithmic axis scale.

irrespective of the starting activator, at ~5% of all sites in the simulation box. Lloyd et al.[37] reported that the silica content in fly ash- and fly ash/slag-based geopolymer pore solutions is less than ~10 mM, which would correspond to ~1% of all sites in the simulation, but also did not observe a clear trend in their concentration data as a function of system composition. Although these numbers do not agree precisely, the differences may be attributed either to the difficulties associated with pore solution extraction and ICP analysis for silica (which tends to form colloids during analysis), the presence of some calcium in the experimental samples leading to a reduction in silica solubility, and/or the inherent limitations of CGMC analysis, such as the absence of long-range interactions and directional bonding.

The percentage of aluminate monomers present in each geopolymer gel system is shown in Figure 1b as a function of the extent of reaction. The gel systems begin with all the alumina sites present as part of the metakaolin. As the reaction progresses, these alumina sites are released into solution, and some participate in polymerization. In order to interpret this Figure accurately, the total percentage of alumina sites in each system needs to be known. For the hydroxide-activated system, the total percentage of occupied sites containing alumina is 50.0% compared with 39.9% for the hydroxide/silicate-activated system and 33.3% for the silicate-activated system. Thus, 63% of the alumina sites in system H exist as monomers in the final configuration, compared to 44% for H/S, and 29% for S. Hence, as the silica content in the activating solution increases, the final percentage of alumina present as monomers decreases, which indicate that the extent of polymerization (cluster formation) has increased.

The aluminate monomer results agree qualitatively with previously reported trends in the literature, where monomeric aluminate species ($Al(OH)_4^-$(aq)) were present at a significant concentration after 7 days of curing in hydroxide-activated metakaolin samples. However, this species was only detectable using ^{27}Al MAS NMR in samples containing less than half the concentration of silica of system H/S here,[38] although its concentration also decreases as a function of curing time and so the more silica-rich samples may show some $Al(OH)_4^-$ in solution if measured at younger ages. As seen in Figure 1b, there are some monomeric alumina species existing in solution in system S after 7,000,000 iterations. However, the percentage observed in this system corresponds to only 3.1% of all sites in the lattice, compared with 7.4% in system H. Hence, although there is not an exact agreement between these simulations and the previously reported literature, the general trend measured experimentally is replicated here using CGMC analysis.

Metakaolin dissolution

The preferential release of aluminum, leading to silica-enriched undissolved particles, has been reported during the initial stages of aluminosilicate dissolution (including for metakaolin) at high pH by numerous authors[39–42] and has been identified during geopolymer formation based on NMR data and statistical thermodynamic modeling.[43] For each system studied in this investigation, the alumina content of the remnant metakaolin particle (initially 50% Al) has been calculated from the simulated box environment after 40,000 iterations, to enable direct analysis of whether the model is able to describe this behavior. For the hydroxide-activated system, the percentage of sites in metakaolin existing as aluminate sites after 40,000 iterations is 45%, and for hydroxide/silicate activation, this percentage is 44 and 42% for silicate activation. Provis et al.[43] estimated from deconvolution of the ^{29}Si MAS NMR spectra of geopolymer gel binders that the remnant metakaolin in their samples was around 40% aluminate, and the simulation results agree well with this estimated value.

Hence, the DFT/CGMC model presented in this investigation does describe the general trend reported previously in the literature regarding the behavior of metakaolin during dissolution, where the initial stages of dissolution consist mainly of aluminum being released from the strained sites in its Al layers, leaving a silica-enriched remnant particle. However, the DFT/CGMC model does not explicitly simulate diffusion of alumina and silica species, apart from the initial and end states, which mean that the alumina (and silica) species will dissolve from all surfaces of the metakaolin particle. These results prove that although the implementation of metakaolin in the simulation methodology does not precisely replicate the coordination environment of metakaolin (four- and five-coordinated sites are present in metakaolin compared to the six-coordination used here), the data obtained do provide a detailed and correct understanding of the mechanisms occurring during metakaolin dissolution.

Visualization

Images of the Monte Carlo simulation box at various stages during the reaction process are displayed in Figures 2–4. Figure 2 displays the clusters present in the hydroxide-activated system during the simulation. Figure 2a (iteration zero) shows the initial metakaolin particle, which subsequently undergoes dissolution, releasing monomeric species, which are able to polymerize to form small clusters (as seen in Figure 2b after 40,000 iterations). As the reaction progresses to 400,000 iterations, the metakaolin particle has dissolved further, and by 4,000,000, it has dissolved completely (as will be explicitly shown in the next section).

Comparison of Figure 2b with Figure 3b (for system H/S) shows that there are more clusters forming in system H/S at 40,000 iterations compared with the hydroxide-activated system (H). This is expected because there are silicate monomers and oligomers initially present in solution in system H/S,[2] which are able to form clusters between themselves and with the aluminum released from metakaolin. The silicate-activated system S (Figure 4b) shows extensive cluster formation after only 40,000 iterations.

The clusters formed at 400,000 and 7,000,000 iterations in the various systems are displayed in Figures 2c/d, 3c/d, and 4c/d. These images reveal increasing densification in the gels with increasing silica content.

Cluster size evolution

Figure 5 displays the percentage of occupied sites which are located within clusters for all gel systems, as a function of the extent of reaction. This Figure quantifies the behavior previously noted in the visualizations given in Figures 2–4, where the systems containing a higher percentage of silica have higher degrees of polymerization at 400,000 and 7,000,000 iterations. Also shown in this Figure is the small percentage of occupied sites in the hydroxide-activated system which exist in clusters after 4,000,000 iterations. This corresponds to the presence of a large percentage of monomers (especially aluminate monomers), as was previously

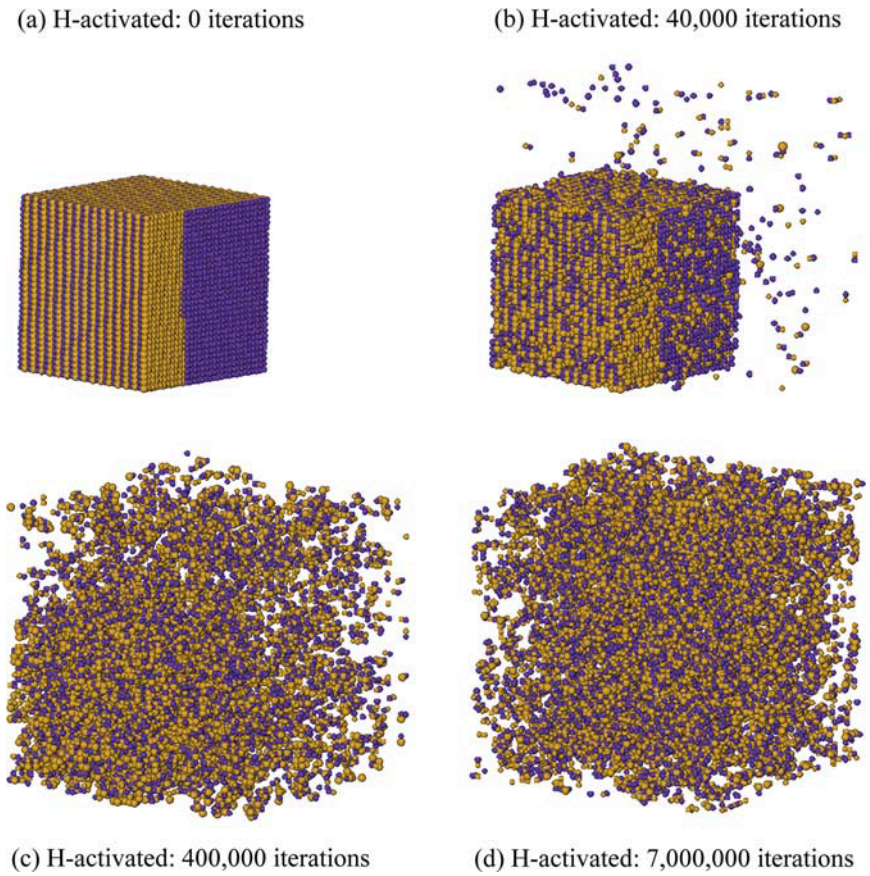

Figure 2. Three-dimensional images of the clusters present in the hydroxide-activated (H) geopolymer gel at various stages (number of iterations) during the simulation.

The metakaolin particle is the only cluster present at the beginning of the simulation (iteration 0), as displayed in (a). Yellow spheres represent silicate sites and purple spheres are aluminate sites. [Color figure can be viewed in the online issue, which is available at wileyonlinelibrary.com.]

shown in Figures 1a and b. These results correlate well with experimentally determined pore volumes in metakaolin-based geopolymers,[44,45] where, on increasing Si/Al ratio, the pore volume decreased and the gel became more space-filling.

Information regarding the structural changes occurring during geopolymerization can be obtained by studying the cluster size development during the simulations. Experimental techniques have generally been unable to provide direct evidence of cluster development during geopolymerization due to the high solid/liquid ratios in these systems, and therefore, simulations are essential in understanding the molecular changes in these systems. Previous modeling work has elucidated important structural information regarding the process of geopolymerization using a reaction kinetic model,[3] where chemical speciation was used to describe coordination states ranging from Q^0 to Q^4, and rate expressions for reactions were developed assuming that the stoichiometry of the reaction predicts the kinetics. However, that methodology did not provide spatially resolved information, which is obtained for the first time in the work presented here.

Figures 6–8 display the cluster size distributions for the hydroxide-activated, hydroxide/silicate-activated, and silicate-activated systems, respectively. Comparison of Figures 6a, 7a, and 8a reveals that, after equilibration, system H contains more occupied sites situated in small clusters (less than 20 sites) than the other systems investigated and, in particular, a higher percentage of dimers. Furthermore, during the reaction, the percentage of dimers in system H increases to a constant value by 400,000 iterations, whereas the silicate-activated system S shows a maximum in the percentage of dimers at 40,000 iterations, after which time the percentage decreases. These results indicate different mechanisms of gel growth depending on the type of activating solution.

The changes taking place in the metakaolin particle during geopolymerization are depicted in Figures 6b, 7b, and 8b for systems H, H/S, and S, respectively. Figure 6b shows that in the hydroxide-activated geopolymer system the metakaolin particle has completely dissolved within 4,000,000 iterations, indicating that there is no residual metakaolin once the system reaches equilibrium. In the hydroxide/silicate-activated system (Figure 7b), the metakaolin particle is mostly dissolved within 7,000,000 iterations; there is one particle present of size ~5,000 sites, which is identified as a remnant small residual particle of metakaolin but with most Al—O—Al linkages dissolved (<3% of the T—O—T linkages being Al—O—Al, where T represents Si and Al). The silicate-activated geopolymer system presents a different trend in metakaolin dissolution, whereby the metakaolin particle initially undergoes some dissolution, but after a period of time, the solid region identifiable as being derived from the original metakaolin particle begins to grow. This is apparent in Figure 8b, which shows the change in size of the largest particle with the number of iterations, where the particle present after 7,000,000 iterations is larger than the particles

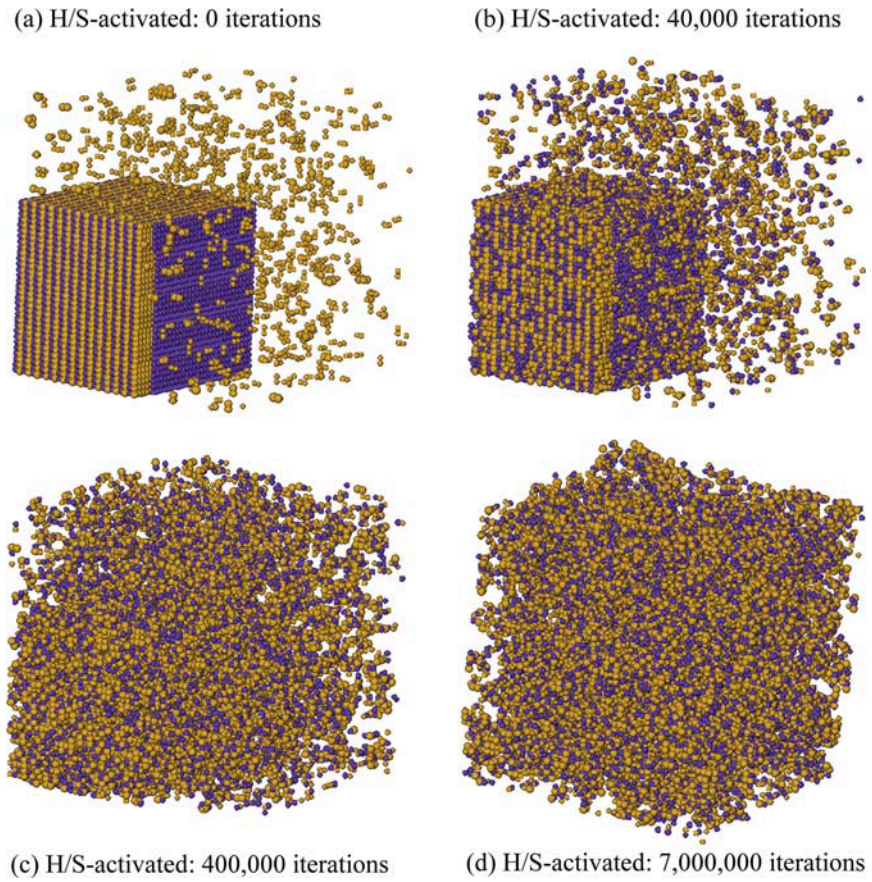

Figure 3. Three-dimensional images of the clusters present in the hydroxide/silicate-activated (H/S) geopolymer gel at various stages (number of iterations) during the simulation.

Yellow spheres represent silicate sites and purple spheres are aluminate sites. [Color figure can be viewed in the online issue, which is available at wileyonlinelibrary.com.]

present at 40,000 and 400,000 iterations. Hence, from the trends reported in these Figures, it can be concluded that the silica content of the activating solutions strongly affects the mechanistic behavior associated with metakaolin dissolution and geopolymer gel growth. Experimentally, it is seen that there is residual metakaolin present in all samples simulated in this investigation,[45] whereas there is no residual metakaolin in the H-activated system presented here. Nevertheless, Duxson et al. reported that the amount of residual metakaolin increases with increasing Si/Al ratio (i.e., moving from the H-activated system to the S-activated).[45] This is also seen in Figures 6b, 7b, and 8b, and therefore, these simulation results agree with the general trend seen experimentally. It should be noted that it is particularly difficult to determine the overall percentage of remnant metakaolin in the systems at equilibrium given that the larger clusters (which contain the metakaolin) tend to be a mixture of remnant metakaolin and gel precipitates. Hence, the exact percentage of metakaolin remaining in the systems has not been calculated.

Provis et al.[46] proposed that there are different mechanisms of gel growth taking place as an alkaline solution interacts with metakaolin particles, depending on the silica content of the solution. For hydroxide-activated systems, it is intuitive that there is a low probability of rapid nucleation close to the surface of metakaolin particles during the initial phase of aluminum dissolution, due to the absence of silica monomers in solution. In system H, as seen in Figure 6b, the metakaolin particle fully dissolves. On the other hand, for silicate-activated system, the soluble silicate supplied by the solution enables the rapid nucleation of aluminosilicate gel particles, which attach to the surface of the metakaolin particle and prevent it from fully dissolving, as seen in Figure 8b. Instead, after a period of time, the particle begins to grow due to polymerization of the alumina and silica monomers, which precipitate as aluminosilicate gel on the surface of the partially dissolved metakaolin particle. This is qualitatively consistent with the solid-state NMR measurements of Duxson et al.,[38] who showed an increasing content of unreacted metakaolin with an increase in silica content in the activator. The importance of nucleation sites in determining aluminosilicate gel structures and connectivity has also been demonstrated for simplified sodium aluminate-geothermal silica geopolymer systems,[47] where manipulation of the silica content of the activating solution was shown to provide control of the extent of gel heterogeneity and local gel Si/Al ratios.

Thus, the previously proposed mechanism of gel growth (nucleation) in metakaolin-based geopolymer systems, and in particular, its dependence on the type of activator used, has been validated and accurately simulated using this DFT/CGMC model. It should be noted that this is quite different from the mechanism of gel growth in fly ash-based geopolymer systems as reported by Lloyd et al.,[48] where silicate-activating solutions enhance the dissolution of the solid aluminosilicate precursor. The reason for this difference between metakaolin and fly ash dissolution behavior during

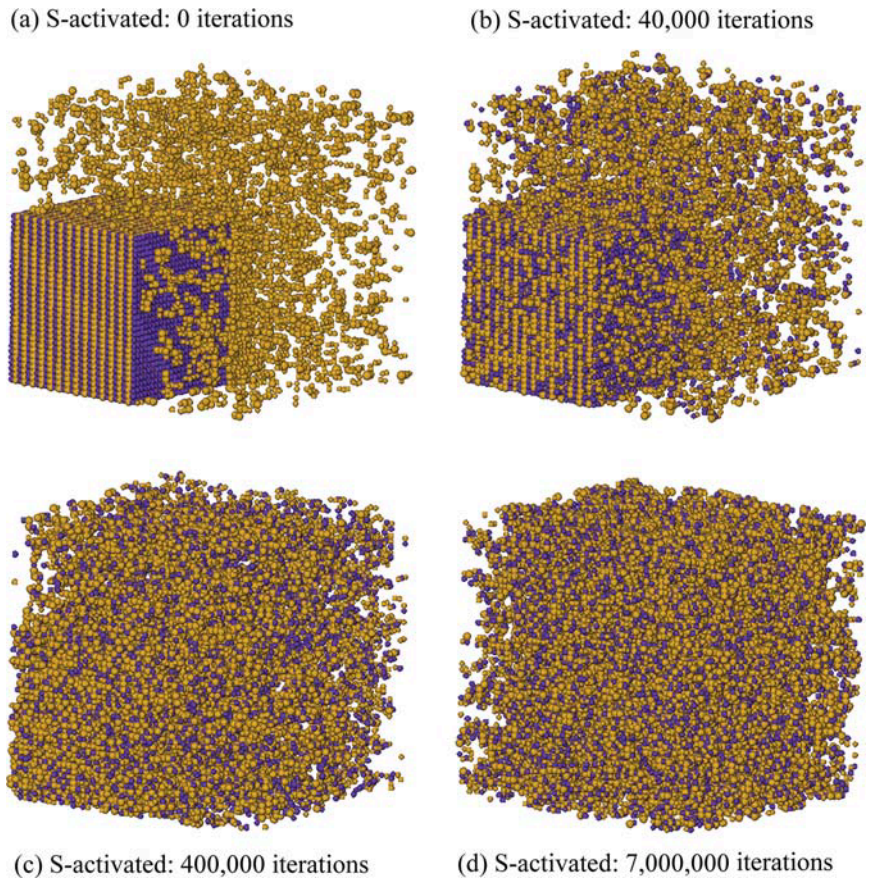

Figure 4. Three-dimensional images of the clusters present in the silicate-activated (S) geopolymer gel at various stages (number of iterations) during the simulation.

Yellow spheres represent silicate sites and purple spheres are aluminate sites. [Color figure can be viewed in the online issue, which is available at wileyonlinelibrary.com.]

geopolymerization is due to the morphology and atomic structure of the precursor material.[49] During hydroxide activation of metakaolin, the layered structure is able to partially exfoliate as interlayer bonds are broken by the early preferential Al release, enhancing further dissolution. On the other hand, during hydroxide activation of fly ash, the spherical glassy aluminosilicate particles release both silica and alumina components, which react to form precipitates on the surface of these spherical particles,[48] thereby hindering further precursor dissolution. Investigating these proposed mechanisms of gel growth, and the differences that are postulated to exist between metakaolin and fly ash-based systems, is possible using the DFT/CGMC methodology.

To further understand the changes happening in the cluster distributions during the reaction, plots displaying the evolution of the size distributions of the smaller clusters formed are given in Figures 9 and 10. Figure 9a displays the cluster size distribution in system H at various stages during the reaction process. As can be seen in this Figure, as the reaction progresses, increasing numbers of smaller ($<$70 sites) clusters form. For system H/S (Figure 9b), there is a distinctly different trend in the evolution of the cluster distribution; after 40,000 iterations, this system shows only very small clusters ($< \sim$20 sites), whereas by 400,000 iterations there exist clusters up to $\sim$50 sites in size. Further polymerization occurs between 400,000 and 7,000,000 iterations, resulting in clusters of up to $\sim$270 sites. Hence, the precipitate units formed in system H/S are larger than those formed in system H. These units are colloidal in size but will probably tend to form gels in the eventual evolution of the final geopolymer structure; there is a consensus in the literature regarding the presence of nanosized gel units within the geopolymer binder, and pair distribution function (PDF) analysis of the geopolymer gel shows gel ordering only on a very short length scale.[50] Furthermore, as shown in Figure 5,

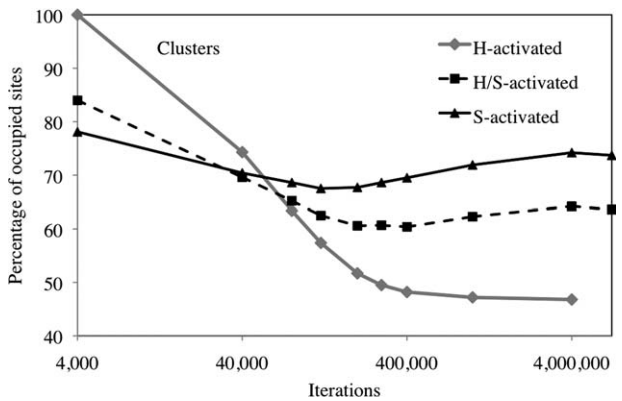

Figure 5. Percentage of occupied sites existing as clusters at various stages during the simulations for the geopolymer gels.

Note that iteration 0 is displayed as iteration 4,000 in the Figure to enable the use of a logarithmic horizontal scale, and that the initial metakaolin particle is classified as a cluster.

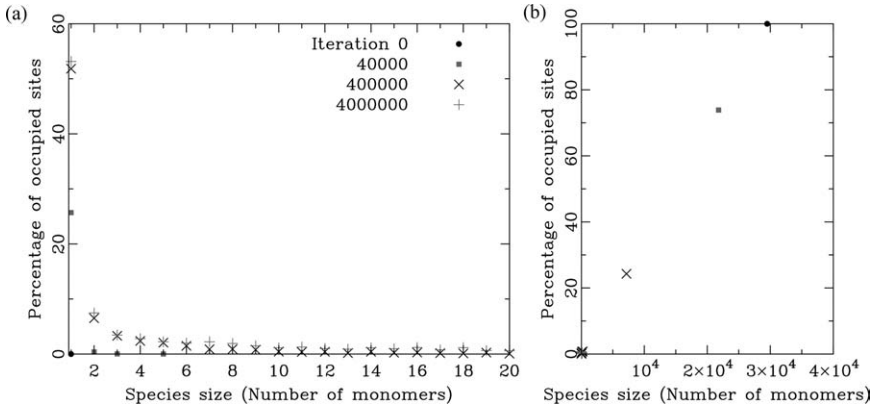

Figure 6. Monomer and cluster size distributions in the hydroxide-activated geopolymer gel at various stages during the simulation, showing (a) the monomers and small clusters and (b) the largest clusters.

63.6% of occupied sites in system H/S are in these precipitates, whereas only 46.8% of sites are in precipitates in system H. This result suggests that the presence of silicate in the activating solution promotes gelation in metakaolin-based geopolymers and aids the formation of larger precipitates, which indicates that a denser gel structure is formed at the nanoscale. Once again, this result agrees with experimental data,[44] where with increasing silica content the pore volume decreased, signifying a more extensive gel network. It should be noted that all systems modeled here form solid binders as seen experimentally.

The changes in the cluster size distribution with increasing extent of reaction in the silicate-activated system S display an Ostwald ripening-type process (Figures 9c and 10c). In this system, as the reaction progresses, the smaller clusters disappear, and there is a preference for growth of larger precipitates at their expense. This is seen in Figures 9c and 10c by the disappearance of small clusters (less than ~50 sites) together with the growth of the largest particle, as previously seen in Figure 8b. Ostwald ripening is a common mechanistic observation in many aqueous silica-based and aluminosilicate-based systems, including silica nanoparticle evolution[33,51] and zeolite formation.[52] It was also observed in our previous DFT/CGMC investigation, where the initial stages of zeolite synthesis were simulated.[2] However, this process has never before been observed during geopolymerization, probably due to the inherent difficulty of experimental elucidation of structural changes occurring in highly alkaline aluminosilicate gels. Hence, the capacity of DFT/CGMC analysis to elucidate such important structural details is especially crucial for the advancement of geopolymer technology. The fact that Ostwald ripening has been observed in the silicate-activated metakaolin geopolymer system but not the others further demonstrates that the silica concentration in the activating solution is critical in dictating how the geopolymer gel evolves.

Nearest-neighbor bonding environment

Previous investigations of metakaolin-based geopolymer binders have suggested that certain alkali-activated systems can contain small percentages of Al—O—Al linkages.[43] These theoretical and experimental results deviate from earlier literature on metakaolin-based geopolymer binders, which assumed that these linkages were completely avoided according to Loewenstein's "rule."[43,53] The current investigation implicitly contains the details of Si—O—Si, Si—O—Al and Al—O—Al bonding within the simulated gel structures, and therefore, this information has been elucidated for the final gels formed (after 4,000,000 or 7,000,000 iterations) for each system, as shown in Figure 11.

Visible in Figure 11 are the nonzero percentages of Al—O—Al linkages in all systems investigated: 4.1% for system H (overall Si/Al ratio of 1.0), 2.6% for H/S (Si/Al = 1.5), and 1.6% for S (Si/Al = 2.0). For hydroxide-activated metakaolin geopolymers, the theoretical investigation

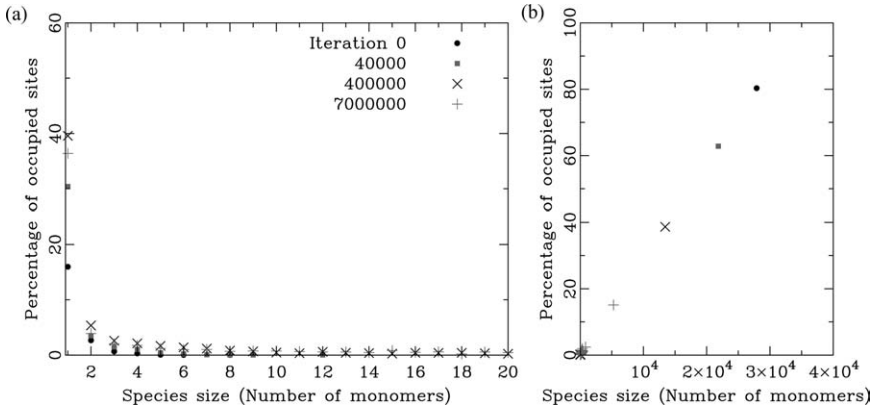

Figure 7. Monomer and cluster size distributions in the hydroxide/silicate-activated geopolymer gel at various stages during the simulation, showing (a) the monomers and small clusters and (b) the largest clusters.

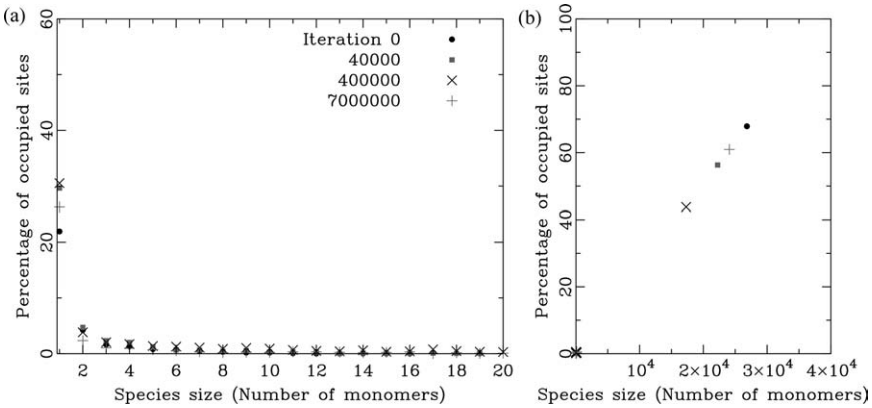

Figure 8. Monomer and cluster size distributions in the silicate-activated geopolymer gel at various stages during the simulation, showing (a) the monomers and small clusters, and (b) the largest clusters.

of Provis et al.[43] determined the percentage of Al—O—Al linkages to be ~1%, with less than 0.1% expected for compositions corresponding to systems H/S and S simulated here. Hence, there is a tendency for the current investigation to report higher percentages of Al—O—Al linkages than are determined experimentally; however, the trend of decreasing percentage with increasing silicon content is evident. As was shown in our previous investigation,[25] the formation of Al—O—Al type dimers is thermodynamically unfavorable, and therefore, structures containing these linkages are weaker at the molecular level when compared with structures containing only Si—O—Si and Si—O—Al linkages. Hence, by tailoring stoichiometry, these linkages can be avoided to ensure stronger nanostructural bonding and better molecular stability of the geopolymer gel material.

Figure 11 also displays the percentages of Si—O—Si and Si—O—Al bond environments for the systems investigated. As the silica content in the activating solution increases, the percentage of Si—O—Si bonds increases while the percentage of Si—O—Al bonds decreases. This is the same trend as was reported by Provis et al.,[43] however, the percentage of Si—O—Si in the hydroxide-activated sample is significantly greater in the current investigation. Reasons for this discrepancy could include the simulation methodology used, as Provis et al.[43] modeled only the Q^4 sites (assuming a fully crosslinked geopolymer gel) and, therefore, did not describe Q^1, Q^2, and Q^3 sites and their associated bonding environments, which are detailed in full in the model presented here.

Aluminosilicate solubility

The solubility product is an important measure of solution chemistry, but for high alkalinity aluminosilicate solutions, this value can be difficult to determine experimentally.[54,55] Šefčík and McCormick reported for sodium aluminosilicate solutions (solutions used to synthesize zeolite A) with sodium concentration between 1 and 4 M, and temperatures between 353 and 363 K, a solubility product ($\Pi_s = [Si(OH)_4][Al(OH)_4^-][Na^+]$) of 1.2 ($\pm 0.3$) $\times$ 10^{-8} M^3.[55] Using this same definition of solubility product for the systems investigated in this study at the end of each simulation, values have been determined; however, these values are necessarily based on systems simulated here at a lower temperature (298.15 K) as defined in the DFT computations used to determine interaction energies. For system H, the solubility product is calculated as 3×10^{-6} M^3, for system H/S the value is 2×10^{-6} M^3, and for system S, the value is $1 \times$

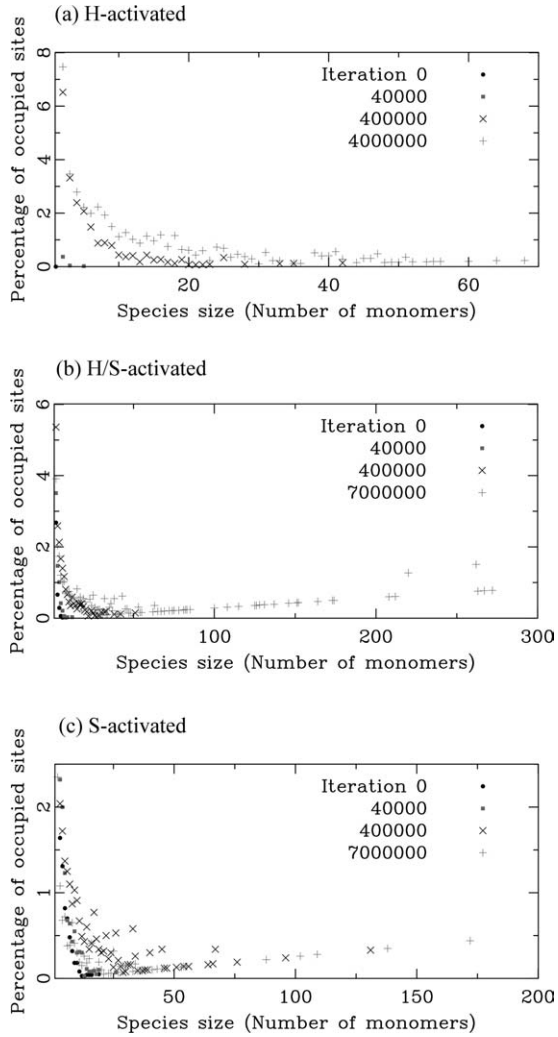

Figure 9. Cluster size distributions of the small clusters (containing less than 300 sites) in the geopolymer gel systems at various stages during the simulations.

(a) Hydroxide-activated system, (b) hydroxide/silicate-activated system, and (c) silicate-activated system.

10^{-6} M^3. Hence, there are a few orders of magnitude separating the solubility product of zeolite A, as calculated by Šefčík and McCormick,[55] and the values obtained in this investigation. However, as was mentioned by Šefčík and McCormick,[55] their investigation was based on experimental data with relatively low concentrations of silica and alumina to maintain monomeric speciation, and therefore, the effect of high silica and alumina concentrations—as is the case for geopolymers—is difficult to elucidate. Furthermore, there is a distinct difference in solubility depending on the phase (crystalline or amorphous), with amorphous aluminosilicates being much more soluble than the crystalline phases of equivalent composition.[56] Hence, the values reported in this investigation provide approximately appropriate solubility product values for the gel products across a range of Si/Al ratios.

Directions for Future Model Development

From the results presented in this investigation, it is evident that molecular modeling, and specifically DFT/CGMC analysis based on quantum chemically determined interaction energies, is a powerful tool capable of elucidating key structural details which would otherwise remain unknown. This article presents the first ever results in the application of this technique to aluminosilicate systems and is restricted to sodium-metakaolin geopolymer binders. Hence, there is much scope for the extension of this model, including analysis of the important and poorly understood role of calcium in geopolymer-forming systems. This study has shown that a material's molecular properties, which are governed by fundamental mechanistic traits, are able to be elucidated using high-level multiscale simulation techniques, which is an important factor for the success of many emerging materials.

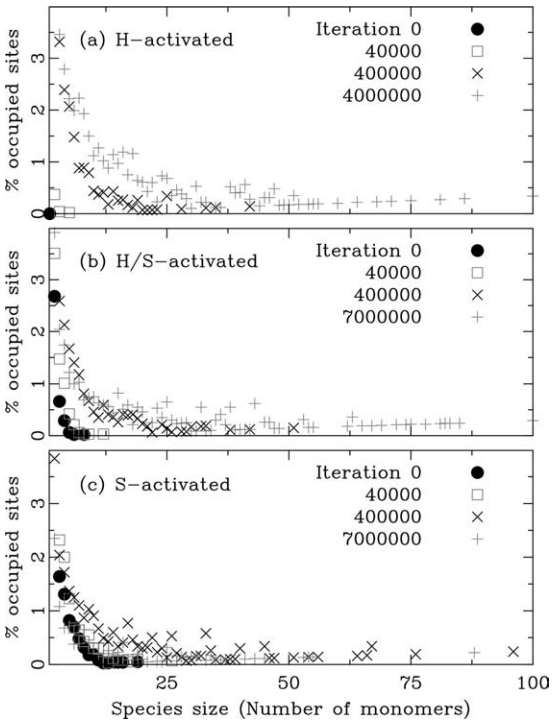

Figure 10. Cluster size distributions of the small clusters (containing less than 100 sites) in the geopolymer gel systems at various stages during the simulations.

(a) Hydroxide-activated system, (b) hydroxide/silicate-activated system, and (c) silicate-activated system.

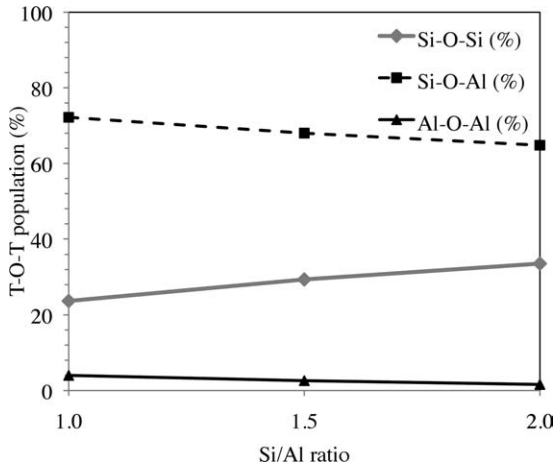

Figure 11. Bond-type distribution in the geopolymer gel systems at the end of each simulation, showing the percentage of Si—O—Si, Si—O—Al, and Al—O—Al bonds.

System H has a Si/Al ratio of 1.0, compared to 1.5 for system H/S and 2.0 for system S.

Conclusions

CGMC simulations, based on interaction energies derived from density functional modeling, have been used to elucidate important structural information regarding metakaolin-based geopolymer binders with sodium as the charge-balancing cation. Three geopolymer systems with varying silica concentrations in their activating solutions have been investigated. The silica content is pivotal in dictating the molecular mechanisms occurring during geopolymerization. As the silica content in the activator of a metakaolin geopolymer system is increased, more species (both aluminate and silicate) participate in polymerization, leading to a denser nanostructure and less monomeric species existing in the pore solution. The precipitates formed become larger with increasing silica content, which indicates that different structural transformation mechanisms occur depending on the type of activator used.

The results of these simulations have confirmed a previously proposed hypothesis regarding nucleation of precipitates in metakaolin-based systems, where in the presence of silicate activating solutions the early release of aluminum from metakaolin leads to localized nucleation close to the surface of the partially dissolved metakaolin particles. On the other hand, in hydroxide-activated systems there is no localized nucleation taking place, and therefore, the precipitates form throughout the system. Furthermore, the results from the silicate-activated system provide direct evidence of Ostwald ripening, which has never before been explicitly shown to occur in geopolymer systems. Hence, this preliminary investigation using DFT/CGMC simulations has shown the power of an accurate modeling technique in elucidating important molecular mechanisms, which are not readily accessible by experimental techniques.

Acknowledgments

This work was funded in part by the Australian Research Council (ARC) (including some funding via the Particulate Fluids Processing Centre, a Special Research Centre of the ARC), and in part by a

studentship paid to Claire White by the Centre for Sustainable Resource Processing via the Geopolymer Alliance.

Literature Cited

1. Duxson P, Provis JL, Lukey GC, van Deventer JSJ. The role of inorganic polymer technology in the development of 'green concrete'. *Cem Concr Res*. 2007;37:1590–1597.
2. White CE, Provis JL, Proffen T, van Deventer JSJ. Quantitative mechanistic modeling of silica solubility and precipitation during the initial period of zeolite synthesis. *J Phys Chem C*. 2011;115:9879–9888.
3. Provis JL, van Deventer JSJ. Geopolymerisation kinetics. 2. Reaction kinetic modelling. *Chem Eng Sci*. 2007;62:2318–2329.
4. Duxson P, Fernández-Jiménez A, Provis JL, Lukey GC, Palomo A, van Deventer JSJ. Geopolymer technology: the current state of the art. *J Mater Sci*. 2007;42:2917–2933.
5. Glukhovsky VD. *Soil Silicate Articles and Structures (Gruntosilikatnye vyroby I konstruktsii)*. Kiev, Ukraine: Budivelnyk Publisher; 1967.
6. Weng L, Sagoe-Crentsil K. Dissolution processes, hydrolysis and condensation reactions during geopolymer synthesis: Part I—Low Si/Al ratio systems. *J Mater Sci*. 2007;42:2997–3006.
7. Rahier H, Wastiels J, Biesemans M, Willlem R, Van Assche G, Van Mele B. Reaction mechanism, kinetics and high temperature transformations of geopolymers. *J Mater Sci*. 2007;42:2982–2996.
8. Zhang YS, Jia YT, Sun W, Li ZJ. Study of ion cluster reorientation process of geopolymerisation reaction using semi-empirical AM1 calculations. *Cem Concr Res*. 2009;39:1174–1179.
9. Zhang YS, Sun W. Semi-empirical AM1 calculations on 6-memebered alumino-silicate rings model: implications for dissolution process of metakaoline in alkaline solutions. *J Mater Sci*. 2007;42:3015–3023.
10. Provis JL, White CE, van Deventer JSJ. Discussion of Y. Zhang et al., "Study of ion cluster reorientation process of geopolymerisation reaction using semi-empirical AM1 calculations," Cem Concr Res 39(12): 1174–1179; 2009. *Cem Concr Res*. 2010;40:827–828.
11. Catlow CRA, George AR, Freeman CM. Ab initio and molecular-mechanics studies of aluminosilicate fragments, and the origin of Lowenstein's rule. *Chem Commun* 1996:1311–1312.
12. Kinrade SD, Pole DL. Effect of alkali-metal cations on the chemistry of aqueous silicate solutions. *Inorg Chem*. 1992;31:4558–4563.
13. Kinrade SD, Swaddle TW. Silicon-29 NMR studies of aqueous silicate solutions. 2. Transverse ^{29}Si relaxation and the kinetics and mechanism of silicate polymerization. *Inorg Chem*. 1988;27:4259–4264.
14. Knight CTG, Balec RJ, Kinrade SD. The structure of silicate anions in aqueous alkaline solutions. *Angew Chem Int Ed Engl*. 2007;46:8148–8152.
15. Kubicki JD, Toplis MJ. Molecular orbital calculations on aluminosilicate tricluster molecules: implications for the structure of aluminosilicate glasses. *Am Mineral*. 2002;87:668–678.
16. Mora-Fonz MJ, Catlow CRA, Lewis DW. Modeling aqueous silica chemistry in alkali media. *J Phys Chem C*. 2007;111:18155–18158.
17. Schaffer CL, Thomson KT. Density functional theory investigation into structure and reactivity of prenucleation silica species. *J Phys Chem C*. 2008;112:12653–12662.
18. Šefčík J, Goddard WA. Thermochemistry of silicic acid deprotonation: comparison of gas-phase and solvated DFT calculations to experiment. *Geochim Cosmochim Acta*. 2001;65:4435–4443.
19. Tossell JA. Theoretical studies on aluminate and sodium aluminate species in models for aqueous solution: $Al(OH)_3$, $Al(OH)_4^-$ and $NaAl(OH)_4$. *Am Mineral*. 1999;84:1641–1649.
20. Zhang L, Luttge A. Aluminosilicate dissolution kinetics: a general stochastic model. *J Phys Chem B*. 2008;112:1736–1742.
21. Rankin SE, Kasehagen LJ, McCormick AV, Macosko CW. Dynamic Monte Carlo simulation of gelation with extensive cyclization. *Macromolecules*. 2000;33:7639–7648.
22. Šefčík J, Rankin SE. Monte Carlo simulations of size and structure of gel precursors in silica polycondensation. *J Phys Chem B*. 2003;107:52–60.
23. Chatterjee A, Vlachos DG, Katsoulakis MA. Spatially adaptive lattice coarse-grained Monte Carlo simulations for diffusion of interacting molecules. *J Chem Phys*. 2004;121:11420–11431.
24. Katsoulakis MA, Vlachos DG. Coarse-grained stochastic processes and kinetic Monte Carlo simulators for the diffusion of interacting particles. *J Chem Phys*. 2003;119:9412–9427.
25. White CE, Provis JL, Kearley GJ, Riley DP, van Deventer JSJ. Density functional modelling of silicate and aluminosilicate dimerisation solution chemistry. *Dalton Trans*. 2011;40:1348–1355.
26. Frenkel D, Smit B. *Understanding Molecular Simulation: From Algorithms to Applications*. San Diego: Academic Press; 1996.
27. Šefčík J, McCormick AV. Thermochemistry of aqueous silicate solution precursors to ceramics. *AIChE J*. 1997;43:2773–2784.
28. Rimer JD, Lobo RF, Vlachos DG. Physical basis for the formation and stability of silica nanoparticles in basic solutions of monovalent cations. *Langmuir*. 2005;21:8960–8971.
29. Caullet P, Guth JL. *Observed and calculated silicate and aluminosilicate oligomer concentrations in alkaline aqueous solutions*. In: Occelli ML, Robson HE, editors. *Zeolite Synthesis*. Washington DC: American Chemical Society; 1989:83–97.
30. White CE, Provis JL, Proffen T, Riley DP, van Deventer JSJ. Combining density functional theory (DFT) and pair distribution function (PDF) analysis to solve the structure of metastable materials: the case of metakaolin. *Phys Chem Chem Phys*. 2010;12:3239–3245.
31. White CE, Provis JL, Proffen T, Riley DP, van Deventer JSJ. Density functional modeling of the local structure of kaolinite subjected to thermal dehydroxylation. *J Phys Chem A*. 2010;114:4988–4996.
32. White CE, Perander LM, Provis JL, van Deventer JSJ. The use of XANES to clarify issues related to bonding environments in metakaolin: a discussion of the paper S. Sperinck et al., "Dehydroxylation of kaolinite to metakaolin-a molecular dynamics study," J Mater. Chem., 2011, 21, 2118–2125. *J Mater Chem*. 2011;21:7007–7010.
33. Jorge M, Auerbach SM, Monson PA. Modeling spontaneous formation of precursor nanoparticles in clear-solution zeolite synthesis. *J Am Chem Soc*. 2005;127:14388–14400.
34. Šomvársky J, Dušek K. Kinetic Monte-Carlo simulation of network formation. II. Effect of system size. *Polym Bull*. 1984;33:377–384.
35. Šomvársky J, Dušek K. Kinetic Monte-Carlo simulation of network formation. I. Simulation method. *Polym Bull*. 1984;33:369–376.
36. Herrmann HJ, Stauffer D, Landau DP. Computer simulation of a model for irreversible gelation. *J Phys A Math Gen*. 1983;16:1221–1239.
37. Lloyd RR, Provis JL, van Deventer JSJ. Pore solution composition and alkali diffusion in inorganic polymer cement. *Cem Concr Res*. 2010;40:1386–1392.
38. Duxson P, Lukey GC, Separovic F, van Deventer JSJ. Effect of alkali cations on aluminum incorporation in geopolymeric gels. *Ind Eng Chem Res*. 2005;44:832–839.
39. Bauer A, Velde B, Berger G. Kaolinite transformation in high molar KOH solutions. *Appl Geochem*. 1998;13:619–629.
40. Kohler SJ, Dufaud F, Oelkers EH. An experimental study of illite dissolution kinetics as a function of pH from 1.4 to 12.4 and temperature from 5 to 50°C. *Geochim Cosmochim Acta*. 2003;67:3583–3594.
41. Oelkers EH, Schott J, Devidal JL. The effect of aluminum, pH, and chemical affinity on the rates of aluminosilicate dissolution reactions. *Geochim Cosmochim Acta*. 1994;58:2011–2024.
42. Walther JV. Relation between rates of aluminosilicate mineral dissolution, pH, temperature, and surface charge. *Am J Sci*. 1996;296:693–728.
43. Provis JL, Duxson P, Lukey GC, van Deventer JSJ. Statistical thermodynamic model for Si/Al ordering in amorphous aluminosilicates. *Chem Mater*. 2005;17:2976–2986.
44. Duxson P, Lukey GC, van Deventer JSJ. Physical evolution of Na-geopolymer derived from metakaolin up to 1000 °C. *J Mater Sci*. 2007;42:3044–3054.
45. Duxson P, Provis JL, Lukey GC, Mallicoat SW, Kriven WM, van Deventer JSJ. Understanding the relationship between geopolymer composition, microstructure and mechanical properties. *Colloids Surf A*. 2005;269:47–58.
46. Provis JL, Lukey GC, van Deventer JSJ. Do geopolymers actually contain nanocrystalline zeolites? A reexamination of existing results. *Chem Mater*. 2005;17:3075–3085.
47. Hajimohammadi A, Provis JL, van Deventer JSJ. The effect of silica availability on the mechanism of geopolymerisation. *Cem Concr Res*. 2011;41:210–216.
48. Lloyd RR, Provis JL, van Deventer JSJ. Microscopy and microanalysis of inorganic polymer cements. 2: The gel binder. *J Mater Sci*. 2009;44:620–631.
49. White CE, Provis JL, Llobet A, Proffen T, van Deventer JSJ. Evolution of local structure in geopolymer gels: an in-situ neutron pair distribution function analysis. *J Am Ceram Soc*. In press; DOI: 10.1111/j.1551–2916.2011.04515.x.

50. White CE, Provis JL, Proffen T, van Deventer JSJ. The effects of temperature on the local structure of metakaolin-based geopolymer binder: a neutron pair distribution function investigation. *J Am Ceram Soc*. 2010;93:3486–3492.
51. Provis JL, Vlachos DG. Silica nanoparticle formation in the TPAOH-TEOS-H_2O system: a population balance model. *J Phys Chem B*. 2006;110:3098–3108.
52. Navrotsky A. Energetic clues to pathways to biomineralization: precursors, clusters, and nanoparticles. *Proc Natl Acad Sci USA*. 2004;101:12096–12101.
53. Loewenstein W. The distribution of aluminum in the tetrahedra of silicates and aluminates. *Am Mineral*. 1954;39:92–96.
54. Gasteiger HA, Frederick WJ, Streisel RC. Solubility of aluminosilicates in alkaline solutions and a thermodynamic equilibrium model. *Ind Eng Chem Res*. 1992;31:1183–1190.
55. Šefčík J, McCormick AV. What is the solubility of zeolite A? *Micropor Mater*. 1997;10:173–179.
56. Addai-Mensah J, Li J, Rosencrance S, Wilmarth W. Solubility of amorphous sodium aluminosilicate and zeolite A crystals in caustic and nitrate/nitrite-rich caustic aluminate liquors. *J Chem Eng Data*. 2004;49:1682–1687.

Manuscript received Apr. 22, 2011, and revision received Jun. 26, 2011.